Desalination and Water Treatment
www.deswater.com

doi: 10.5004/dwt.2020.25696

190 (2020) 12–27
June

Modeling self-sustainable fully-covered photovoltaic thermal-compound parabolic concentrators connected to double slope solar distiller

Vidya Sagar Gupta[a], Desh Bandhu Singh[b,*], Sanjeev Kumar Sharma[c], Navneet Kumar[a], T.S. Bhatti[d], G.N. Tiwari[e,f]

[a]*Galgotias College of Engineering and Technology, Plot No 1, Knowledge Park II, Greater Noida, G. B. Nagar, 201306, India, emails: vsg60@rediffmail.com (V.S. Gupta), navneet.kumar@galgotiacollege.edu (N. Kumar)*
[b]*Department of Mechanical Engineering, Graphic Era (Deemed to be University), Bell Road, Clement Town, Dehradun – 248002, Uttarakhand, India, emails: dbsiit76@gmail.com/deshbandhusingh.me@geu.ac.in (D.B. Singh)*
[c]*Department of Mechanical Engineering, Amity University, Noida, Uttar Pradesh, India, email: sksharma6@amity.edu (S.K. Sharma)*
[d]*Centre for Energy Studies, Indian Institute of Technology Delhi, HausKhas, New Delhi, 110016, India, email: tsb@ces.iitd.ac.in (T.S. Bhatti)*
[e]*Research and Development Cell, Shri Ramswaroop Memorial University (SRMU), Lucknow-Dewa Road, (UP), 226028, India, email: gntiwari@ces.iitd.ernet.in (G.N. Tiwari)*
[f]*Bag Energy Research Society (BERS), SODHA BERS COMPLEX, Plot No. 51, Mahamana Nagar, Karaudi, Varanasi, UP, 22 10 05, India*

Received 22 May 2019; Accepted 15 February 2020

ABSTRACT

The present study discusses the development of the characteristic equation of a PVT (photovoltaic thermal)-CPC (compound parabolic concentrator collector) for $N = 6$ similar fully covered incorporated with solar distiller unit in a very scientific manner similar to the equation of Hottel–Whillier–Bliss equation for FPC (flat plate collector). There are certain drawbacks in partially covered PVT collectors like (a) low thermal behavior because of the high top loss coefficient, (b) higher maintenance of the system, and (c) costly manufacturing. Due to these problems, $N = 6$ similar fully covered PVT-CPC incorporated with solar distiller system have been considered in the present study. The analytical expression for the proposed system has been established by means of scripting equations for balancing energy for its different elements (present study, case (i)). The instantaneous efficiency of the proposed system has been computed using a computational program in MATLAB. The system performance of proposed $N = 6$ same fully covered PVT-CPC incorporated with solar distiller unit (double slope-active) is being matched with (case (ii)) N identical Fully covered PVT-FPCs incorporated with solar distiller system (double slope-active), (case (iii)) conventional $N = 6$ same FPC incorporated with solar still (double slope-passive), and (case (iv)) passive solar still with a double slope. During the comparison, it has been observed that instantaneous efficacy is higher in case (i) when compared with case (ii), and case (iv), but lower than case (iii).

Keywords: Photovoltaic thermal (fully covered) – compound parabolic concentrator; Double slope solar distiller unit; Characteristic equation

1. Introduction

The solar distiller unit can be broadly categorized as passive and active. The problem of low output of a passive system is fully addressed in an active system. The study of solar still (active) is one the substitute for the energy crisis and water crisis in the economically developing nation. The literature study highlights much experimental work carried out earlier. Zaki et al. [1] was first to report that solar stills behave in dynamic manner when the mode of circulation

* Corresponding author.

is natural whereas a pump (motor) was used for uniform circulation of water in the pipe. There is an increase in the evaporation rate when heat transfer is increased. As per Rai and Tiwari [2], when the operation is in forced mode then the active solar stills give 24% higher yield with one collector while matching with solar distiller unit (conventional). In solar distiller unit (active), a pump is connected in the middle of the inlet of the first collector which is connected in series with other collectors and the basin.

Basin in solar distiller unit (active) consists of FPC/evacuated concentrator collector or tube collector/heat exchanger which is used to supply thermal energy from other sources. In general, a heat exchanger uses water as liquid whereas other fluids may also be used as per the requirement. Abdel-Rehim and Lasheen [3] have worked on the same by incorporating heat exchanger and solar parabolic trough collector on solar still (single slope). Solar still of conventional type has less output efficiency by 18% when it was compared with the solar parabolic trough collector on the distiller system. The improvement is only due to the increase in the temperature of water in the distiller system of single slope type (SS) because of an increase in water temperature in the basin. Transportation of heat takes place to the bottom of SS by circulating the fluid in SS which in turn also increases the yield. If the rate of heat transfer is doubled then 9% increase in yield was found [4]. It has been found that the relation between the production of potable water and the rate of heat transfer is not linear. In the forced mode of operation of double slope solar active still, the yield was found to be 52% higher [5] while comparing the production with conventional type solar still. When flat plate collector (FPC) was integrated with solar still having a higher depth of water, the thermal efficiency, and exergy were found to be more and also the yield was more because of sensible heat storage in the water [6]. In European Mediterranean nations, Calise et al. [7] proposed a technologically advanced framework by using photovoltaic thermal (PVT) collectors for desalinating hard water. Ibrahim et al. [8] improved the distiller system with the integration of cooling condensers outside while comparing with conventional type solar still. It was found 16.2% rise in yield and 29.7% rise in thermal efficiency.

Active solar distiller system integrated with FPC can be made self-sustainable when the distiller is connected with photovoltaic panel in order to provide thermal energy as well as electrical energy which can be used for our many domestic purposes. A hypothetical investigation of such a framework by Hendrie [9,10] showed that the electrical energy obtained could be improved by allowing the water to flow below the PV panel. Guarracino et al. [11] reported the testing of hybrid PVT solar collectors and concluded that the thermal response of PVT collector is slower than that of FPC under dynamic test condition. Mellor et al. [12] have presented strategies for reducing convective, radiative and electrical losses at elevated temperature. Liang et al. [13] studied a new type of PVT solar collector containing graphite experimentally and concluded that the electrical efficiency of new type collectors was 20.28% higher than the electrical efficiency of conventional PVT collector because of better cooling effect. He et al. [14] studied PVT collector experimentally in natural circulation mode and concluded that the daily electrical efficiency was around 10%. As per Kumar and Tiwari [15–18], one partially covered FPCs with PV module connected (series) with other FPCs when coupled with solar distillation system was found to give an increase in yield by 3.5 times than solar still (conventional type). Further, it was stated that the payback time for the solar unit coupled with FPC (in series) would be between 3.9 and 23.9 y. Singh et al. [19] studied the same and worked on double slope solar still (active).

Saeedi et al. [20] used mathematical calculation for mass flow rate and with seven number of collectors for PVT active SS and obtained ideal values for rate of mass flow as 0.044kg/s. Singh and Tiwari [21–24] and Prasad et al. [25] performed a theoretical analysis on single slope as well as double slope solar distillation system when incorporated with N identical PVT-CPC (compound parabolic concentrator) collectors for Delhi climatic condition. It was found that the double slope set up was better than the single slope of the same configuration at 0.14 m water depth conditions of optimization because of higher exergy, energy and low embodied energy for set up having a double slope. Further, the researchers proposed that a single slope system having a water depth greater than 0.31 m, the system could give better results as compared with the double slope in terms of daily average yield, thermal efficiency, and overall thermal performance. Singh et al. [26,27] and Singh and Tiwari [28] reported characteristic equation development for basin type solar still coupled with evacuated tubular collectors.

Gaur and Tiwari [29] observed that the basin of the solar distiller system when incorporated with N FPCs having a water mass of 50 kg, based on exergy effectiveness, number of collectors should be four. When solar still (single slope) consist of FPC, showering unit as well as external condenser, it was found an increase in yield from 51% to 148% while relating it to solar distiller (conventional type) [30]. In research work done by Rabhi et al. [31] on solar distiller unit (single slope) integrated with condenser and pin fins, the yield was found to be 41.98% more when compared with conventional solar still and also the temperature of the water in the distiller increases. Sharshir et al. [32] investigated that solar distillation system of hybrid in nature (humidification–dehumidification), the yield increases by 200% while relating it to solar distiller (conventional type).

Navarro et al. [33] reported the analysis of a double slope solar distiller unit for three materials using the Energy2D computer program and concluded that heat loss is less when polyurethane was used. Sharma et al. [34] developed a characteristic equation of concentrator integrated evacuated tubular collector and coupled with a double slope solar distiller unit. They concluded that the double slope solar still coupled with concentrator integrated evacuated tubular collector performs better than that of double slope solar still integrated with evacuated tubular collector due to the presence of concentrator which concentrates the solar energy on the receiver surface. Haiping et al. [35] studied experimentally a flash tank coupled with low concentrating photovoltaic hybrid system for getting freshwater and concluded that the maximum electrical power and freshwater obtained on a typical day were 447.55 W and 23.65 kg, respectively.

From the current literature survey, it is observed that the development of characteristic equation, energy, and

exergy analysis has not been yet explored for a fully covered PVT-CPC joined with solar distiller (double slope) by any researcher for same watt peak as PVT-FPC (partly covered) combined with solar still.

Demerits of the PVT-FPC (partly covered with PVT)/CPC collector (partly covered with PVT) combined solar still (double slope) is given below:

- Low thermal behavior due to heat loss from the glazed portion of the PVT-FPC (partly covered with PVT)/CPC collector (partly covered with PVT).
- Manufacturing of the system is costly.
- System needs high maintenance which requires frequent cleaning of the top portion of the PV module.

So this paper describes the specific equations for PVT-CPC collector combined with solar distiller (double slope).

Drawback mentioned above has been fully described for the equal watt peak. So in this paper, we have developed a characteristic equation for N identical PVT-CPC which is fully covered and integrated with double slope solar distiller unit followed by the computation of energy and exergy. Further, the developed equation is also suitable for:

- PVT-FPC combined with solar distiller unit (double slope)
- Conventional FPC integrated with solar distiller unit of double slope type and
- Passive solar still of double slope type.

2. Modeling methodology

Fig. 1 describes the present work and its specification has been tabulated in Table 1. The Fig. 2a shows the cut section view and representation of N-identical PVT-CPC (fully covered) combined with a solar distiller unit (double slope). When collectors are collected in parallel, low-temperature yield is found to be more and when connected in series for high temperature the yield is less. In the proposed work, all the collectors are connected in series with solar still to increase the temperature of the saline water.

In the present study, the basin water is fed to the inlet of the first fully covered PVT-CPC by a motor pump. The output of the fully covered PVT-CPC is fed to the input of the second PVT-CPC connected in series and so on. The output of nth connected PVT CPC is fed to the inlet of the basin. Hence, the temperature of the water in the basin is increased by many folds. So in this system, the concept of closed-loop has been described. All collectors connected in series are inclined to an angle of 30° to achieve the maximum annual radiation from the sun. The motor pump gets supply from the PVT system and it always maintains the uniform circulation of water through the pipeline of the system.

A glass (reinforced plastic) is fitted at the top of the basin having an effective area of 2 m^2. The transparent glass functioning as a condensing cover is inclined at 15° and solar still is positioned in the east-west direction as shown in Fig. 2a. The inside and outside portion of solar still has been painted with black color to absorb maximum solar flux. The joint of glass with the basin has been sealed with a putty cover. The basin has been facilitated with the two connections. One at the side top connected to the outlet of the nth PVT-CPC and other at the bottom connected to the inlet of the motor pump. The solar still have another opening at the bottom for cleaning purpose and solar still system is placed rigidly on a frame made of iron (steel).

When the solar radiation falls on the top surface of the glass cover (installed over the solar steel), a part of solar flux is reflected, another absorbed and remaining radiation is transmitted to the basin water. An upper surface of the water further reflects a part of solar flux, another absorbed, and rest of the flux is transmitted to the bottom of the basin. So, the radiation received by the basin liner will, in turn, increase

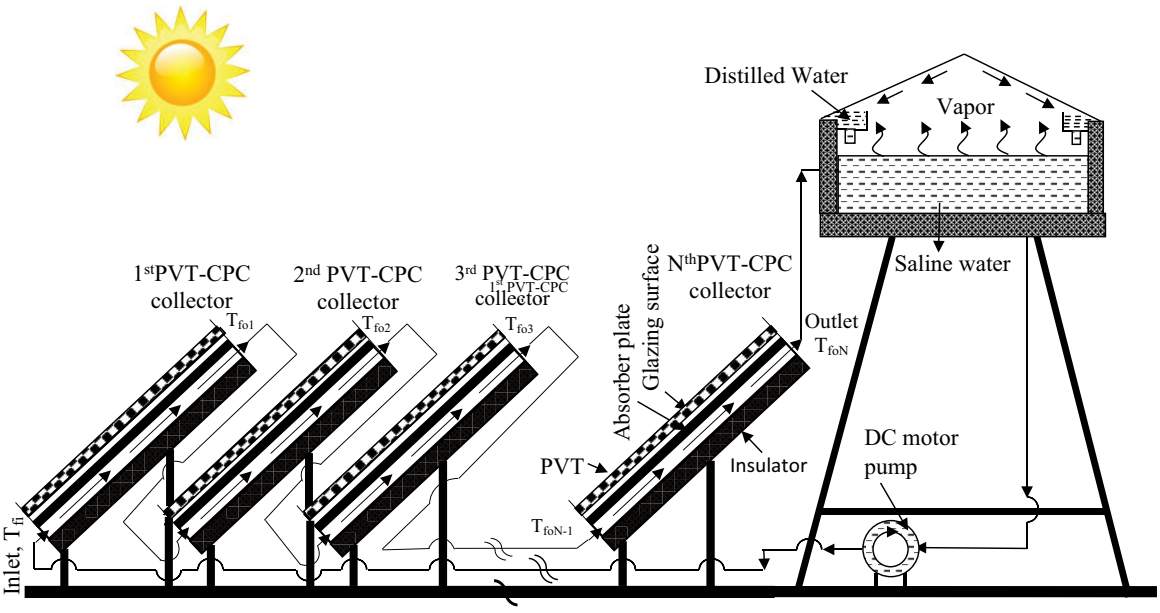

Fig. 1. Schematic diagram of proposed N identical fully covered PVT-CPC integrated double slope solar distiller unit.

Table 1
Specifications of *N* identical fully covered PVT-CPC integrated double slope solar distiller

Double slope solar still			
Component	Specification	Component	Specification
Length	2 m	Material of body	GRP
Width	1 m	Material of stand	GI
Inclination of east glass cover	15°	Cover material	Glass
Inclination of west glass cover	15°	Orientation	East–West
Height of smaller side	0.2 m	L_i	0.1 m
K_g	0.816 W/m-K	K_i	0.166 W/m-K
L_g	0.004 m		
Fully covered PVT-CPC collector			
Component	Specification	Component	Specification
Type and no of collectors	Tube in plate type, *N*	Aperture area	2 m^2
Receiver area of solar water collector	1.0 m × 1.0 m	Aperture area of collector	1.0 m× 2.0 m
Collector plate thickness	0.002	α_p	0.8
Thickness of copper tubes	0.00056 m	FF	0.85
Length of each copper tubes	1.0 m	Receiver area of collector	1.0 m × 1.0 m
Angle of CPC with Horizontal	30°	F''	0.968
DC motor rating	12 V, 24 W	ρ	0.84
β_c	0.22	τ_g	0.95
Pipe diameter	0.0125 m	α_c	0.9

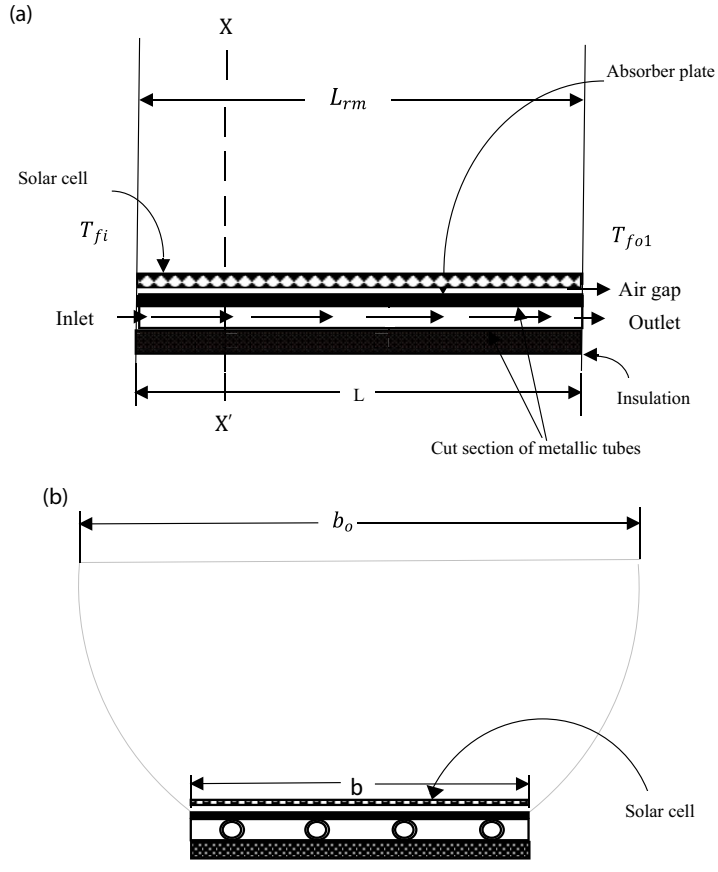

Fig. 2. (a) Cross-section side view of proposed fully covered PVT-CPC collector. (b) Cut section XX′ front view of fully covered PVT-CPC collector.

the temperature of the saline water in addition to the heated water received from the output of *N* PVT-CPC. Now, the process of evaporation takes place inside the basin due to the temperature difference between the bottom/inner surface of the glass cover and the saline water in the basin. The evaporated water starts condensing at the inner portion of the condensing cover which further drops down and collected in a container placed externally.

To analyze the system, we consider the subsequent assumptions given as below:

- Quasi-steady-state conditions are considered for the proposed active distillation system.
- Between the two solar cells, the ohmic losses are ignored.
- Temperature gradient remains unchanged around the PV module as well as insulating material used.
- The heat flow in one direction has been considered.
- There is no vapor leakage in solar distiller.
- The basin has a fixed level of saline water.
- The evaporation gets condensed upon the bottom surface of the condensing cover.

2.1. Equations for different components of the proposed system

2.1.1. Energy balance equations for solar cell of PV module

When the solar radiation are incident on the solar cell of the PV module, a part of solar flux is reflected, another part absorbed and the rest of solar flux is transmitted through it to the plate. A part of solar flux absorbed by the solar cell is converted into DC electrical power by the photovoltaic effect. Other part of absorbed solar flux is wastage to the surroundings and the rest of the solar flux is transferred to the collectors. Following is the energy balance equation for the solar cell of the PV module.

$$\rho\alpha_c\tau_g\beta_c I_b A_{\text{am}} = \left[U_{\text{tca}}\left(T_c - T_a\right) + U_{\text{tcp}}\left(T_c - T_p\right)\right]A_{\text{rm}} + \rho\eta_m I_b A_{\text{am}} \quad (1)$$

The term ($\rho\alpha\tau_g\beta_c I_b A_{\text{am}}$) in the left-hand side of Eq. (1) describes the rate of beam radiation falling on the solar cell and the first term $[U_{\text{tca}}(T_c - T_a)]A_{\text{rm}}$ in right-hand side of the expression shows the rate of heat loss from solar cell to the atmosphere, the second term $[U_{\text{tcp}}(T_c - T_p)]A_{\text{rm}}$ shows the rate of heat transfer from the solar cell to absorber plate and the third term $\rho\eta_m I_b A_{\text{am}}$ express conversion of solar radiation into direct current.

Eq. (1) can be rewritten in terms of T_c as follows:

$$T_c = \frac{\left(\alpha\tau\right)_{\text{1eff}} I_b + U_{\text{tca}}T_a + U_{\text{tcp}}T_p}{U_{\text{tca}} + U_{\text{tcp}}} \quad (2)$$

2.1.2. Energy balance equation for absorber plate

The heat transfer from plate to fluid is specified by indirect gain (solar cell to plate through convection and radiation) as well as direct gain (through the non-packing area of the module). It has been described by the following equation:

$$\rho\alpha_p\tau_g^2\left(1-\beta_c\right)I_b A_{\text{am}} + U_{\text{tcp}}\left(T_c - T_p\right)A_{\text{rm}} = F'h_{\text{pf}}\left(T_p - T_f\right)A_{\text{rm}} + U_{\text{tpa}}\left(T_p - T_a\right)A_{\text{rm}} \quad (3)$$

The first term [$\rho\alpha\ \rho\tau_g^2\ (1-\beta_c)I_b A_{\text{am}}$] and the second term [$U_{\text{tcp}}(T_c - T_p)A_{\text{rm}}$] on the left side of Eq. (3) shows the direct gain (through non-packing area) as well as indirect gain to the plate.

The subsequent terms [$F'h_{\text{pf}}(T_p - T_f)A_{\text{rm}} + U_{\text{tpa}}(T_p - T_a)A_{\text{rm}}$] on the right side of the Eq. (3) shows the rate of heat transfer (plate to fluid) and the heat loss (plate to surrounding) per unit time, respectively.

Eqs. (2) and (3) can be rewritten in term of T_p (plate temperature) as follows:

$$T_p = \frac{\left[\left(\alpha\tau\right)_{\text{2eff}} + \text{PF}_1\left(\alpha\tau\right)_{\text{1eff}}\right]I_b + U_{L2}T_a + h_{\text{pf}}T_f}{\left(U_{L2} + h_{\text{pf}}\right)} \quad (4)$$

Appendix-A contains $(\alpha\tau)_{\text{2eff}}$, $(\alpha\tau)_{\text{1eff}}$, PF_1, U_{L2}, h_{pf}, U_{tp}, U_{ta}, and U_{tpa}.

2.1.3. Water/fluid flowing through the pipe

The heat transfer from absorber plate to fluid is carried away through the pipe. So the energy balance equation (referring to Fig. 2a) for flowing fluid has been written as follows:

$$\dot{m}_f C_f \frac{dT_f}{dx}\text{dx} = F'h_{\text{pf}}\left(T_p - T_f\right)b\ dx \quad (5)$$

The first term $\left(\dot{m}_f C_f \frac{dT_f}{dx}dx\right)$ on the left side of Eq. (5) shows heat transported to water per unit time, the term [$F'h_{\text{pf}}(T_p - T_f)\ bdx$] shows heat transfer from absorber plate to water/fluid per unit time.

Modifying Eq. (5) with the help of Eq. (2) as well as Eq. (4)

$$\dot{m}_f C\frac{dT_f}{dx}dx = bF'\left[I_b\text{PF}_2\left(\alpha\tau\right)_{m,\text{eff}} - U_{\text{Lm}}\left(T_f - T_a\right)\right]dx \quad (6)$$

The value of collector efficiency factor (F') can be evaluated by Duffie and Beckman [36] and Tiwari [37].

Initial condition is considered to obtain solution for Eq. (6) is $T_f|_{x=0} = T_{\text{fi}}$ and can be expressed as:

$$T_f = \left[\frac{\text{PF}_2\left(\alpha\tau\right)_{\text{meff}} I_b}{U_{\text{Lm}}} + T_a\right]\left[1 - \exp\left\{\frac{-bF'U_{\text{Lm}}x}{\dot{m}_f c_f}\right\}\right] + T_{\text{fi}}\exp\left[\frac{-bF'U_{\text{L,m}}x}{\dot{m}_f c_f}\right] \quad (7)$$

Hence, the output fluid temperature of the first collector is given below:

$$T_{\text{fo1}} = \left[\frac{\text{PF}_2\left(\alpha\tau\right)_{m,\text{eff}} I_b}{U_{\text{Lm}}} + T_a\right]\left[1 - \exp\left\{\frac{-F'U_{\text{Lm}}A_{\text{rm}}}{\dot{m}_f C_f}\right\}\right] + T_{\text{fi}}\exp\left[\frac{-F'U_{\text{Lm}}A_{\text{rm}}}{\dot{m}_f C_f}\right] \quad (8)$$

In the same way, the temperature of the water at the second collector output will be in relations to input water temperature is given as:

$$T_{\text{fo2}} = \left[\frac{\text{PF}_2(\alpha\tau)_{\text{m,eff}} I_b}{U_{\text{Lm}}} + T_a\right]\left[1-\exp\left\{\frac{-F'U_{\text{Lm}}A_{\text{rm}}}{\dot{m}_f C_f}\right\}\right] + T_{\text{fi2}}\exp\left[\frac{-F'U_{\text{Lm}}A_{\text{rm}}}{\dot{m}_f C_f}\right] \quad (8b)$$

Here, assumptions made are as follows:

- PVT collectors have same area
- $U_{t,\text{pa}}$ overall heat transfer coefficient (plate to ambient) is same

As, $T_{\text{fi2}} = T_{\text{fo1}}$, water temperature at the inlet of the second PVT-CPC is equal to the outlet water temperature of first PVT-CPC. As all N collectors are connected in series as stated earlier, T_{fo2} can be further rewritten as:

$$T_{\text{fo2}} = \left[\frac{(\text{PF})_2(\alpha\tau)_{\text{meff}} I_b}{U_{\text{Lm}}} + T_a\right]\left[\frac{(2)(A_m F_{\text{Rm}})U_{\text{Lm}}}{\dot{m}_f C_f}\right] + T_{\text{fi}}\left[1-\frac{(2)(A_m F_{\text{Rm}})U_{\text{Lm}}}{\dot{m}_f C_f}\right] \quad (8c)$$

where,

$$(A_m F_{\text{Rm}}) = \frac{\dot{m}_f C_f}{U_{\text{Lm}}}\left[1-\exp\left(-\frac{F'U_{\text{Lm}}A_{\text{rm}}}{\dot{m}_f C_f}\right)\right] \quad (8d)$$

Appendix-A defines the various term used in the Eqs. (1)–(8d). It has already been explained that all PVT-CPC are connected in series. It means water outlet of first PVT-CPC is fed to the input of the second PVT-CPC and water output of second PVT-CPC is fed to the inlet of third PVT-CPC and so on. The output water of nth PVT-CPC is circulated to the basin through the pipe. So the temperature of water at the outlet is written below:

$$T_{\text{foN}} = \left[\frac{(PF)_2(\alpha\tau)_{\text{meff}} I_b}{U_{\text{Lm}}} + T_a\right]\left[\frac{N(A_m F_{\text{Rm}})U_{\text{Lm}}}{\dot{m}_f C_f}\right] + T_{\text{fi}}\left[1-\frac{N(A_m F_{\text{Rm}})U_{\text{Lm}}}{\dot{m}_f C_f}\right] \quad (9)$$

For N identical fully covered PVT-CPCs, the useful heat gain ($\dot{Q}_{\text{uN}}$) can be expressed as:

$$\dot{Q}_{\text{uN}} = \dot{m}_f C_f (T_{\text{foN}} - T_{\text{fi}}) \quad (10)$$

Using Eqs. (9) and (10), $\dot{Q}_{\text{uN}}$ can be expressed as:

$$\dot{Q}_{\text{uN}} = N(A_m F_{\text{Rm}})\left[(\text{PF})_2(\alpha\tau)_{\text{meff}} I_b - U_{\text{Lm}}(T_{\text{fi}} - T_a)\right] \quad (11)$$

An analytical expression by Evans [38] and Schott [39] for electrical solar cells efficiency (η_{cN}) is as follows:

$$\eta_{\text{cN}} = \eta_0\left[1-\beta_0(\bar{T}_{\text{cN}} - T_0)\right] \quad (12)$$

where η_0 = efficiency (standard test condition)
$\bar{T}_{\text{cN}}$ = average temperature of solar cell
The electrical energy (varied hourly) can be written as:

$$\dot{E}_{\text{elec}} = A_m I_b(t)\sum_1^N(\beta_c\tau_g\eta_{cN}) \quad (13)$$

2.2. Energy balance equation for different parts of the active solar still (double slope)

2.2.1. Bottom portion of the glass cover facing towards east

When sunlight incidents on the upper portion of the glass cover surface from eastern side, a part of radiant flux is reflected back, another gets absorbed and the rest of the solar flux is transported to basin water. The bottom surface of glass cover also gets heat energy from the upper surface of the water by a process of evaporation, convection, and radiation. Due to difference in temperature between water and bottom surface of glass, then the loss of heat occurs to the condensing cover (bottom portion to upper portion by the process of conduction). Thus, the equation defines the energy balance for the bottom portion of the condensing cover as follows:

$$\alpha'_g I_{\text{SE}}(t)A_{\text{gE}} + h_{\text{1wE}}(T_w - T_{\text{giE}})\frac{A_b}{2} - h_{\text{EW}}(T_{\text{giE}} - T_{\text{giW}})A_{\text{gE}} = \frac{K_g}{L_g}(T_{\text{giE}} - T_{\text{goE}})A_{\text{gE}} \quad (14)$$

The first term of Eq. (14) on LHS signifies the rate at which the solar energy is being absorbed by glass cover facing east, the second term of Eq. (14) on LHS signifies the amount of heat received from the water surface by the process of convection, radiation, and evaporation and the third term signifies the rate of heat loss to glass cover facing west from glass cover facing east. The term on right-hand side of the Eq. (14) shows loss of energy from bottom to upper portion of glass (facing east) through the transmission.

2.2.2. Upper portion of condensing cover (facing east)

The upper portion of the condensing cover (facing east) gets the solar energy through conduction from glass cover inner surface facing east and loss of heat occurs through convection and radiation, to ambient by glass cover facing east. Hence, the equation of energy balance for glass cover outer surface facing east can be expressed as:

$$\frac{K_g}{L_g}(T_{\text{giE}} - T_{\text{goE}})A_{\text{gE}} = h_{\text{1gE}}(T_{\text{goE}} - T_a)A_{\text{gE}} \quad (15)$$

where h_{1gE} denotes total HTC to ambient through the process of convection and radiation from glass cover outer surface

facing east. The expression of Eq. (15) on LHS signifies heat transferred from glass cover inner surface facing east to glass cover outer surface facing east. The term on the left-hand side of the equation signifies the transfer of heat through conduction from bottom surface of the condensing cover to a top portion facing towards east. The term on the right-hand side equation signifies the loss of heat from the top surface of glass (facing east) to the surrounding atmosphere by conduction and radiation.

2.2.3. Glass cover inner surface (facing towards west)

When sunlight incident on the upper portion of the glass cover surface from the western side, a part of radiant flux is reflected back, another gets absorbed and the rest of the solar flux is transported to basin water. The bottom portion of condensing cover gets heat energy from the upper portion of the water by a process of evaporation, convection, and radiation. Loss of heat occurs from the bottom portion to upper portion of the condensing cover through conduction. Thus, the equation defines the energy balance for the bottom portion of the condensing cover as follows:

$$\alpha'_g I_{\mathrm{SW}}\left(t\right)A_{\mathrm{gW}} + h_{1\mathrm{wW}}\left(T_w - T_{\mathrm{giW}}\right)\frac{A_b}{2} + h_{\mathrm{EW}}\left(T_{\mathrm{giE}} - T_{\mathrm{giW}}\right)A_{\mathrm{gE}} = \frac{K_g}{L_g}\left(T_{\mathrm{giW}} - T_{\mathrm{goW}}\right)A_{\mathrm{gW}} \tag{16}$$

The term $[\alpha'_g I_{\mathrm{SW}}(t)A_{\mathrm{gW}}]$ on LHS of Eq. (16) signifies absorptivity of radiation flux by condensing cover (facing west); the next term $\left[h_{1\mathrm{wW}}\left(T_w - T_{\mathrm{giW}}\right)\frac{A_b}{2}\right]$ of Eq. (16) on left hand side signifies energy obtained by condensing cover (facing west) from the fluid in the basin. The third term $[h_{\mathrm{EW}}(T_{\mathrm{giE}} - T_{\mathrm{giW}})A_{\mathrm{gE}}]$ on left hand side of Eq. (16) defines the energy gain by the glass cover facing west from glass cover facing east. The term $\left[\frac{K_g}{L_g}\left(T_{\mathrm{giW}} - T_{\mathrm{goW}}\right)A_{\mathrm{gW}}\right]$ on right-hand side of Eq. (16) shows the heat loss from the bottom portion of the glass cover (facing west) to its upper portion by a process of conduction.

2.2.4. Upper portion of the glass cover (facing west)

The upper portion of the glass cover (facing west) receives heat through conduction from glass cover inner surface facing west and heat is lost through convection and radiation, to ambient by glass cover facing west. Hence, the equation of energy balance for glass cover outer surface facing west can be expressed as:

$$\frac{K_g}{L_g}\left(T_{\mathrm{giW}} - T_{\mathrm{goW}}\right)A_{\mathrm{gW}} = h_{1\mathrm{gW}}\left(T_{\mathrm{goW}} - T_a\right)A_{\mathrm{gW}} \tag{17}$$

where $h_{1\mathrm{gW}}$ denotes total HTC to ambient through the process of convection and radiation from glass cover outer surface facing west. The term on the left-hand side of Eq. (17) signify the transfer of heat through conduction from the bottom surface of the condensing cover to top portion facing towards west. The term on the right-hand side equation signifies the loss of heat from top surface of glass (facing west) to the surrounding atmosphere by conduction and radiation.

2.2.5. Energy balance equation for the basin liner

The basin liner of the solar still has been painted with black color to absorb the maximum solar radiation transmitted by upper portion of the water to the basin liner. The basin liner, in turn, raises the water temperature by a process of convection. The heat loss also takes place from the bottom as well as a side portion of the basin liner to the surroundings through insulation.

$$\alpha'_b\left(I_{\mathrm{SE}}\left(t\right) + I_{\mathrm{SW}}\left(t\right)\right)\frac{A_b}{2} = h_{\mathrm{bw}}\left(T_b - T_w\right)A_b + h_{\mathrm{ba}}\left(T_b - T_a\right)A_b \tag{18}$$

The first term $\left[\alpha'_b\left(I_{\mathrm{SE}}\left(t\right) + I_{\mathrm{SW}}\left(t\right)\right)\frac{A_b}{2}\right]$ of Eq. (18) on left-hand side signifies the rate at which the basin liner absorbs solar energy. The first term $[h_{\mathrm{bw}}(T_b - T_w)A_b]$ of Eq. (18) on right-hand side defines the transfer of heat (basin liner to water) and the heat loss basin liner to ambient is defined by the next term $[h_{\mathrm{ba}}(T_b - T_a)A_b]$ of the equation.

2.2.6. Energy balance equation for the mass of basin water

There is a direct heat gain by the water mass from the sun as well as from the basin liner. There is also indirect energy received by the mass of water from outlets of the nth PVT-CPC collector. So the heat gain by the water mass in the basin increases the difference of the temperature between basin water and the inner surface of both the condensing cover (east and west) and causing the process of evaporation to take place. The following equation defines the gain and loss of heat energy by the mass of basin water.

$$\left(M_w C_w\right)\frac{dT_w}{dt} = \left(I_{\mathrm{SE}}\left(t\right) + I_{\mathrm{SW}}\left(t\right)\right)\alpha'_w\frac{A_b}{2} + h_{\mathrm{bw}}\left(T_b - T_w\right)A_b - h_{1\mathrm{wE}}\left(T_w - T_{\mathrm{giE}}\right)\frac{A_b}{2} - h_{1\mathrm{wW}}\left(T_w - T_{\mathrm{giW}}\right)\frac{A_b}{2} + \dot{Q}_{uN} \tag{19}$$

Here, $\dot{Q}_{\mathrm{uN}}$ = the rate thermal energy (output nth collector PVT-CPCs) as defined in Eq. (11). The term on the left-hand side of Eq. (19) signifies how the water mass gains the heat. The first term $\left[\left(I_{\mathrm{SE}}\left(t\right) + I_{\mathrm{SW}}\left(t\right)\right)\alpha'_w\frac{A_b}{2}\right]$ of Eq. (19) in the right-hand side signifies the absorptivity of heat by the mass of the water, the next term $[h_{\mathrm{bw}}(T_b - T_w)A_b]$ of Eq. (19) signifies heat convection to mass of the water from basin liner. The next term $\left[h_{1\mathrm{wE}}\left(T_w - T_{\mathrm{giE}}\right)\frac{A_b}{2}\right]$ of Eq. (19) on the right-hand side of Eq. (19) signifies the loss of heat to the bottom portion of condensing cover (facing east) from the mass of the water, and the term $\left[h_{1\mathrm{wW}}\left(T_w - T_{\mathrm{giW}}\right)\frac{A_b}{2}\right]$ of signifies the rate at which the heat is lost to glass cover inner surface facing west from water

mass and the fifth term [$\dot{Q}_{uN}$]of Eq. (19) on RHS signifies the rate of heat gain from collectors.

Eq. (19) can be written as:

$$\frac{K_g}{L_g}\left(T_{\text{giE}}-T_{\text{goE}}\right)A_{\text{gE}}=U_{\text{cE}}\left(T_{\text{giE}}-T_a\right)A_{\text{gE}} \tag{20}$$

where,

$$U_{\text{cE}}=\frac{\frac{K_g}{L_g}h_{1\text{gE}}}{\frac{K_g}{L_g}+h_{1\text{gE}}} \tag{20a}$$

Using Eqs. (14) and (20), one can get:

$$\alpha_g' I_{\text{SE}}(t)A_{\text{gE}}+h_{1\text{wE}}\left(T_w-T_{\text{giE}}\right)\frac{A_b}{2}-h_{\text{EW}}\left(T_{\text{giE}}-T_{\text{giW}}\right)A_{\text{gE}}= U_{\text{cE}}\left(T_{\text{giE}}-T_a\right)A_{\text{gE}} \tag{21}$$

Similarly, using Eqs. (16) and (17), one can get:

$$\alpha_g' I_{\text{SW}}(t)A_{\text{gW}}+h_{1\text{wW}}\left(T_w-T_{\text{giW}}\right)\frac{A_b}{2}+h_{\text{EW}}\left(T_{\text{giE}}-T_{\text{giW}}\right)A_{\text{gW}}= U_{\text{cW}}\left(T_{\text{giW}}-T_a\right)A_{\text{gW}} \tag{22}$$

where,

$$U_{\text{cW}}=\frac{\frac{K_g}{L_g}h_{1\text{gW}}}{\frac{K_g}{L_g}+h_{1\text{gW}}} \tag{22a}$$

Using Eqs. (21) and (22), one can get:

$$T_{\text{giW}}=\frac{C_1+C_1'+T_w\left(h_{1\text{wE}}\frac{A_b}{2}+h_{1\text{wW}}\frac{A_b}{2}\right)-T_{\text{giE}}\left(h_{1\text{wE}}\frac{A_b}{2}+U_{\text{cE}}A_{\text{gE}}\right)}{h_{1\text{wW}}\frac{A_b}{2}+U_{\text{cW}}A_{\text{gW}}} \tag{23}$$

Eq. (23) can further be rearranged using T_w as:

$$\left(T_w-T_{\text{giW}}\right)=\frac{T_w\left(U_{\text{cW}}A_{\text{gW}}-h_{1\text{wE}}\frac{A_b}{2}\right)-C_1-C_1'+T_{\text{giE}}\left(h_{1\text{wE}}\frac{A_b}{2}+U_{\text{cE}}A_{\text{gE}}\right)}{h_{1\text{wW}}\frac{A_b}{2}+U_{\text{cW}}A_{\text{gW}}} \tag{24}$$

Eq. (23) can also be rearranged using T_{giE} as:

$$\left(T_{\text{giE}}-T_{\text{giW}}\right)=\frac{T_{\text{giE}}\left(h_{1\text{wE}}\frac{A_b}{2}+h_{1\text{wW}}\frac{A_b}{2}+U_{\text{cE}}A_{\text{gE}}+U_{\text{cW}}A_{\text{gW}}\right)-C_1-C_1'-T_w\left(h_{1\text{wE}}\frac{A}{2}+h_{1\text{wW}}\frac{A}{2}\right)}{h_{1\text{wW}}\frac{A_b}{2}+U_{\text{cW}}A_{\text{gW}}} \tag{25}$$

where C_1 and C_1' are given in Appendix-A.

Using Eqs. (22)–(25), T_{giE} can be evaluated as:

$$T_{\text{giE}}=\frac{A+BT_w}{H} \tag{26}$$

Expressions for *A*, *B*, and *H* are specified in Appendix-A.

Putting the value of T_{giE} in Eq. (23) and rearranging various terms, one can get the expression for T_{giW} as:

$$T_{\text{giW}}=\frac{A'+B'T_w}{H} \tag{27}$$

Expressions for *A′* and *B′* are given in Appendix-A.

Eq. (18) can be expressed as:

$$2h_{\text{bw}}\left(T_b-T_w\right)\frac{A_b}{2}=\alpha_b' h_1 A_b\left(I_{\text{SE}}(t)+I_{\text{SW}}(t)\right)-U_b A_b\left(T_w-T_a\right) \tag{28}$$

Using Eqs. (19) and (26)–(28), one can get the following differential equation:

$$\frac{dT_w}{dt}+aT_w=f(t) \tag{29}$$

where,

$$a=\left\{\left(\frac{A_b}{2H}\right)\left(\frac{1}{M_w C_w}\right)\right\}\left[h_{1\text{wE}}\left(E_1+E_2\right)+h_{1\text{wE}}\left(E_1'+E_2'\right)+H_{22}'\right] \tag{30}$$

$$f(t)=\left\{\left(\frac{A_b}{2H}\right)\left(\frac{1}{M_w C_w}\right)\right\}\begin{bmatrix}\left(K_{1E}+\alpha_{\text{wb}}\right)I_{\text{SE}}(t)+\left(K_{1W}+\alpha_{\text{wb}}\right)\\ I_{\text{SW}}(t)+T_a\left(H_{11}'+H_{22}'\right)+\left(\frac{2H}{A_b}\right)\\ N\left(A_m F_{\text{Rm}}\right)\left(\text{PF}\right)_2\left(\alpha\tau\right)_{\text{meff}}I_b(t)\end{bmatrix} \tag{31}$$

Expressions for various terms used Eqs. (30) and (31) are given in Appendix-A.

Using Eq. (29) one gets the differential equation as follows:

$$T_w=\frac{\bar{f}(t)}{a}\left(1-e^{-at}\right)+T_{w0}e^{-at} \tag{32}$$

where T_{w0} represents the value of T_w at t = 0 and $\bar{f}(t)$ represents the average value of $f(t)$ between time interval 0 and t.

The evaporative heat transfer rate expressed as:

$$\dot{q}_{\text{ew}}=\left[h_{\text{ewE}}\left(T_w-T_{\text{giE}}\right)+h_{\text{ewW}}\left(T_w-T_{\text{giW}}\right)A_b\right] \tag{33}$$

Appendix-A contains all the terms used in the equation.

The value of the hourly yield is given below:

$$\dot{m}_{\text{ew}}=\frac{\dot{q}_{\text{ew}}\times 3{,}600}{L} \tag{34}$$

For the proposed system, the instantaneous thermal efficiency (η_i) expressed as:

$$\eta_i = \frac{\dot{q}_{ew}}{NA_{am}I_b(t) + A_{gE}I_{SE}(t) + A_{gW}I_{SW}(t)} = \frac{[h_{ewE}(T_w - T_{giE}) + h_{ewW}(T_w - T_{giW})A_b}{NA_{am}I_b(t) + A_{gE}I_{SE}(t) + A_{gW}I_{SW}(t)} \quad (35)$$

The definition of the instantaneous efficiency assumes that there are no dynamic effects and that no energy is stored in the collector which has a very fast thermal response. Substituting the value of T_{giE} from Eq. (26) and T_{giW} from Eq. (27) in Eq. (35), one can get:

$$\eta_i = \left(\frac{A_b}{H}\right)\frac{\left[\left\{h_{ewE}(H-B) + h_{ewW}(H-B')\right\}T_w - \left\{h_{ewE}A + h_{ewW}A'\right\}\right]}{\left[NA_{am}I_b(t) + A_{gE}I_{SE}(t) + A_{gW}I_{SW}(t)\right]} \quad (36)$$

Expressions for A, A', B, B', and H are given in Appendix-A.

In Eq. (36), substituting the value of T_w from Eq. (32) and rearranging, one can get:

$$\eta_i = \left(\frac{A_b}{H}\right)\left[\frac{1}{\left\{NA_{am}I_b(t) + A_{gE}I_{SE}(t) + A_{gW}I_{SW}(t)\right\}}\right] \left[\begin{array}{l} \left\{h_{ewE}(E_1+E_2) + h_{ewW}(E_1'+E_2')\right\}\left\{\begin{array}{l}\frac{\bar{f}(t)}{a}\left(1-e^{-at}\right)+\\ T_{w0}e^{-at}\end{array}\right\} \\ -\left(K_{1E}'I_{SE}(t) + K_{1W}'I_{SW}(t)\right) - T_a\left\{\begin{array}{l}h_{ewE}(E_1+E_2)+\\ h_{ewW}(E_1'+E_2')\end{array}\right\} \end{array}\right] \quad (37)$$

Substituting values of $\bar{f}(t)$ and a in Eq. (37) and rearranging, one can get:

$$\eta_i = \left(\frac{A_b}{H}\right)\left[\frac{1}{\left\{NA_{am}I_b(t) + A_{gE}I_{SE}(t) + A_{gW}I_{SW}(t)\right\}}\right] \left[\begin{array}{l} \left\{\frac{h_{ewE}(E_1+E_2) + h_{ewW}(E_1'+E_2')}{H_{11}'+H_{22}'}\right\} \\ \left\{\left\{\left\{\left(K_{1E}+\alpha_{wb}\right)I_{SE}(t) + \left(K_{1W}+\alpha_{wb}\right)I_{SW}(t)+\right\}\right.\right. \\ \left.\left.\left\{\left(\frac{2H}{A_b}\right)N\left(A_mF_{Rm}\right)(PF)_2(\alpha\tau)_{meff}I_b(t)\right\}\right. \\ \left.\left(1-e^{-at}\right)\right\} - \left\{K_{1E}'I_{SE}(t) + K_{1W}'I_{SW}(t)\right\}e^{at} \\ +\left(T_{w0}-T_a\right)\left(H_{11}'+H_{22}'\right)e^{-at} \end{array}\right] \quad (38)$$

Expressions for E_1, E_2, E_1', E_2', K_{1E}', and K_{1W}' are given in Appendix-A.

Eq. (38) can further be expressed as:

$$\eta_i = F_{1g}'\left[\begin{array}{l}\frac{X_{11}Y_{11} - \left\{K_{1E}'I_{SE}(t) + K_{1W}'I_{SW}(t)\right\}e^{at}}{\left\{NA_{am}I_b(t) + A_{gE}I_{SE}(t) + A_{gW}I_{SW}(t)\right\}} + \\ \left(H_{11}'+H_{11}'\right)\frac{(T_{w0}-T_a)}{\left\{NA_{am}I_b(t) + A_{gE}I_{SE}(t) + A_{gW}I_{SW}(t)\right\}}\end{array}\right] \quad (39)$$

where,

$$X_{11} = \frac{h_{ewE}(E_1+E_2) + h_{ewW}(E_1'+E_2')}{H_{11}'+H_{22}'};\ F_{1g}' = \left(\frac{A_b}{H}\right)e^{-at};$$

$$Y_{11} = \left\{\begin{array}{l}\left(K_{1E}+\alpha_{wb}\right)I_{SE}(t) + \left(K_{1W}+\alpha_{wb}\right)I_{SW}(t)+\\ \left(\frac{2H}{A_b}\right)N\left(A_mF_{Rm}\right)(PF)_2(\alpha\tau)_{meff}I_b(t)\end{array}\right\}\left(e^{-at}-1\right);$$

$$\alpha_{wb} = \left(\alpha_w' + 2\alpha_b'h_1\right)H$$

Expressions for H, H_{11}', and H_{22}' are given in Appendix-A. In Eq. (39):

- If $A_{am} = A_{rm}$; $\rho = 1$; $I_b(t) = I(t)$, we can get the solution for the same number of completely covered PVT-FPC connected with distiller system (double slope).
- If $A_{am} = A_{rm}$; $\rho = 1$; $I_b(t) = I(t)$; and β is zero. Under this condition, we can get the solution for same number of FPCs connected with distiller system (double slope).
- If $A_m = 0$, then we can get a typical equation for passive double slope solar still.

2.3. Methods for solution of the equations

- *Step i*: Knowing the value of T_{wo}, T_{gi0E}, and T_{gi0W}, and the obtained average values $\bar{I}(t)$, $\bar{I}_b$ and $\bar{T}_a$, water temperature (T_w) can be calculated for climatic conditions and design parameters from Eq. (32). After evaluating T_w from Eq. (32), values of T_{giE} and T_{giW} have been computed using Eqs. (26) and (27), respectively. Then, values of T_{goE} and T_{goW} has been calculated with the help of Eqs. (15) and (17), respectively.
- *Step ii*: Since $T_{fi} = T_w$ (as calculated in step 1), so T_{foN} can be evaluated using Eq. (9) and $\bar{T}_{fn}$ (average water temperature) can be obtained as $\bar{T}_{fN} = \frac{T_{foN} + T_w}{2}$.
- *Step iii*: $\bar{T}_p$ can be calculated from Eq. (4) [after evaluating $\bar{T}_{fn}$ from step-ii], trailed by the calculation of ($\bar{T}_{cN}$) by using Eq. (2) and η_{cN} will be evaluated with the help of Eq. (12).
- *Step iv*: Using Eq. (13) we can find the hourly DC electrical power ($\dot{E}_{elec}$) as well as the entire heat transfer coefficient. Then, the hourly yield ($\dot{m}_{ew}$) can be obtained using Eq. (34).
- *Step v*: By using Eq. (39), η_i (instantaneous efficiency) can be calculated.

3. Experimental validation of *N* alike fully covered PVT-CPCs integrated double slope solar distiller unit

3.1. For N identical fully covered PVT-CPCs connected in series

Tripathi and Tiwari [40] have validated fully covered PVT-CPC collector taking values of *N*, mass flow rate, packing factor and concentration ratio as 1, 0.01 kg/s, 0.89, and 2, respectively. They collected data from 9:00 to 16:00 h on September 21 and 22, 2015. Data was collected for solar intensity, ambient air temperature, tank temperature, cell temperature, and temperature-dependent electrical efficiency. They performed the statistical analysis and found the value of correlation coefficient between theoretical and experimental values as 0.98 for water temperature which represents a fair agreement between theoretical and experimental values.

3.2. For double slope solar distiller unit

Dwivedi and Tiwari [41] have performed the experimental validation of double slope passive solar still for New Delhi climatic condition at different water depths taking basin area as 2 m^2. They have collected data for solar intensity, ambient air temperature, water temperature, condensing cover temperatures, and hourly yield for October 2005–September 2006. They evaluated heat transfer coefficients and hourly yield for April 2006 using various models namely Kumar and Tiwari [42], Dunkle [43], Chen et al. [44], Adhikari et al. [45], Zheng et al. [46], and Clark [47]. They obtained the best result for heat transfer coefficient and hourly yield using Dunkle's model. A fair agreement was found between experimental and theoretical values of hourly yield using Dunkle's model taking percentage error as the basis.

4. Results and discussion

The instantaneous efficiency was obtained out for a specific day in May. The subsequent data (ambient temperature (T_a), Beam radiation (I_b), and Global radiation ($I(t)$)) has been shown on an hourly basis in Fig. 3. The average velocity of air for the May month is 4.02 m/s. The information about solar radiation and ambient temperature has been collected from meteorological sections, Pune (India). For the inclined surface of 30° latitude of the northern hemisphere, the global radiation $I(t)$ and beam radiation I_b have been calculated with the help of the Liu and Jordan technique and MATLAB. The instantaneous efficiency for different specifications, that is, total no. of collectors (N) = 6, mass flow rate = 0.03 kg/s, and water depth = 0.14 m has been calculated. A comparison study has been made among the results of all the three cases (i, ii, iii, and iv).

Fig. 4 shows the module and cell efficiency variation on an hourly basis. Module efficiency was found to be less than the efficiency of the cell for the same packing factor, that is, 0.22. The value of watt peak of fully covered PVT-CPC as well as partly covered connected with distiller system (double slope) remains the same as the number of solar cells and ultimately solar cells area is the same because watt peak remains the same. It is observed from Fig. 4 that the cell as well as module efficiency decreases first and then increases. The solar cell efficiency has been found to be higher in the morning as well as evening. It happens because solar cell temperature is lower in the morning as well as evening due to lower solar intensity. Due to comparatively lower temperatures of solar cells, the emission of electrons is less and collisions among electrons are also less resulting in the higher current generation and hence higher solar cell efficiency. At noon, solar cell efficiency, as well as module efficiency, has been found to be comparatively lower due to higher solar intensities as evident from Figs. 3 and 4. It happens because solar cell temperature is higher due to higher amount of heat available from sun. Due to comparatively higher solar cell temperature, emission of electrons is higher resulting in more collisions among electrons. Due to increased collisions, the current output decreases and hence decreased efficiency is found.

Fig. 5 displays an hourly variation of different temperature for number of collectors (N) = 6, $\dot{m}_f$ = 0.03 kg/s, water depth = 0.14 m. The temperature of water from the outlet of the Nth collector (T_{foN}) is higher than the temperature of water in the solar still because of the uniform circulation of the basin water through the pipe by the motor in the closed-loop system. During the circulation of water through pipes of collectors, water gains heat. When solar radiation impinges on the surface of the first collector, some part is reflected by glass surface, some part is absorbed by the glass surface and the remaining part is transmitted to the solar cell. The solar cell converts some part of radiation coming to it into electrical energy, some part of the radiation is lost to surrounding and the remaining part of the radiation

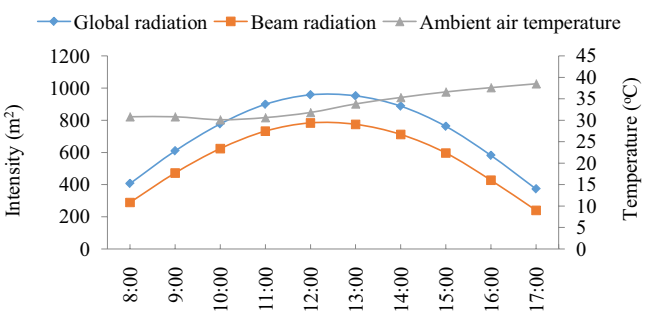

Fig. 3. Hourly variation of intensity and ambient air temperature for a typical day in the month of May.

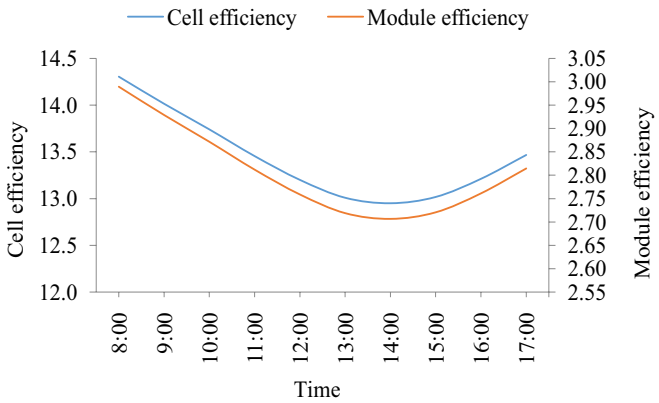

Fig. 4. Hourly variation of cell and module efficiencies.

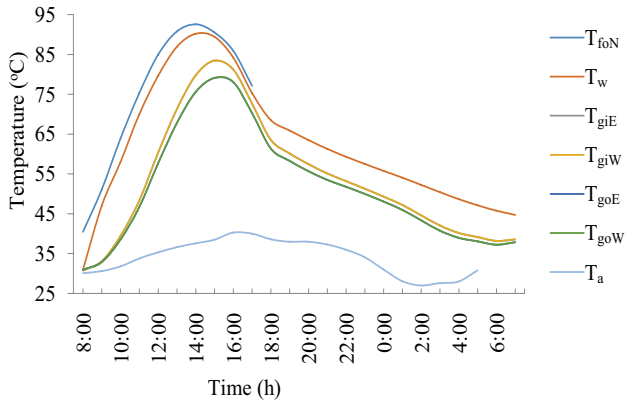

Fig. 5. Hourly variation of temperature of double slope solar still integrated with *N* fully covered PVT-CPC collector connected in series for an archetypal day of May (*N* = 6).

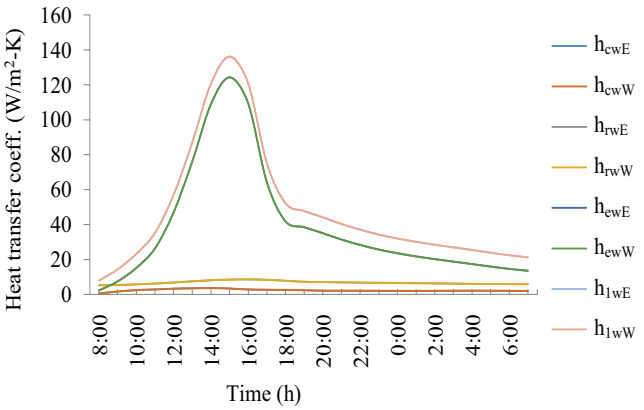

Fig. 6. Hourly variation of heat transfer coefficient of double slope solar still integrated with *N* identical fully covered PVT-CPC collector connected in series for an archetypal day of May (*N* = 6).

is transmitted to the absorber plate. The absorber plate receives indirect radiation through the solar cell and direct radiation through gap between solar cells. The temperature of absorber plate rises due to absorption of both direct and indirect radiation. The absorber plate transmits heat energy to water flowing through tube by heat transfer mechanism. Hence, the temperature of water flowing through the first collector rises due heat gain. The hot water coming out of the first collector is allowed to flow into the second collector as collectors are connected in series. Hot water while passing through second collector gains heat and temperature of water further rises. In this way, heat is gained by water while passing through subsequent collectors. At the end of *N*th collector, the temperature of water at the outlet of *N*th collector is much higher than the temperature at the inlet of first collector. The temperature of water at the outlet of *N*th collector is even higher than the temperature of water in the basin due to heat gain in series connected collectors.

The temperature of water T_w in the tank is also found to be more than the temperature of the glass/condensing cover for the corresponding value (as condensing cover loses heat to the surroundings through the process of convection, radiation, and conduction). Water in the basin receives heat from the collector, direct solar radiation and indirectly from basin liner. For the subsequent value of collectors (*N*) = 6, $\dot{m}_f$ = 0.03 kg/s, depth of water in the basin = 0.14 m, the heat transfer coefficient (on an hourly basis) has been reflected in Fig. 6 for the typical day in the month of May. It has been found that the evaporative heat transfer coefficient is more than convective, as well as the radiative heat transfer coefficient as the process of evaporation rate, is higher than convective and radiative process. The evaporative heat transfer coefficient is higher at 4 pm due to low value of difference in temperature between (T_w – (T_{giE}/T_{giW})). It is noted that convective and radiative heat transfer coefficients are lost to the system whereas evaporative heat transfer coefficient are beneficial to the system (i.e., results in more output).

Fig. 7 reflects the change in instantaneous efficiency (η_i) on an hourly basis for the proposed system at *N* = 6, $\dot{m}_f$ = 0.03kg/s and water depth = 0.14 m for a typical day in the month of May and a comparison study has been made among the system of different cases (i, ii, iii, and iv).

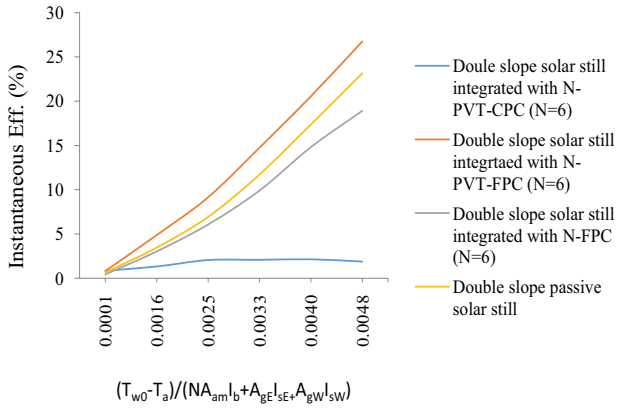

Fig. 7. Comparison of hourly variation of instantaneous efficiency of double slope solar distiller unit integrated with *N*-PVT-CPC/*N*-PVT-FPC/*N*-FPC and passive solar still an archetypal day of May (*N* = 6).

Considering the case (i), the value of instantaneous efficiency (η_i) is more than case (ii) because of the induction of CPC collectors (which is designed efficiently to collect and concentrate the distant light energy) which in turn increases the temperature of the water outlet from the *N*th collector (T_{foN}). Further, it is noted that instantaneous efficiency of conventional *N* = 6 same FPC incorporated with solar still (double slope-passive) is higher than Fully covered PVT-CPC connected with distiller system (double slope) because of the FPCs having more heat exchanging area in absence of PV module. Also, some portion of solar radiation falling on the surface of fully covered PVT-FPC is converted into electrical energy; whereas, solar radiation is not converted into electrical energy in the case of conventional FPC due to the absence of PV. Hence, heat gain by water flowing through conventional FPCs is higher than the heat gain by water flowing through fully covered PVT-FPC. So more heat is transported to the water circulated through the tubes underneath the collector which in turn increase the temperature of the outlet water from *N*th collector (T_{foN}).

The instantaneous efficiency for case (iv) has been found to be lowest. It happens because, there is no external heat source connected to solar distiller as solar distiller is in passive mode. It works on direct heat gain from solar radiation due to the absence of heat source like collector and hence temperature of water in the basin is much lower than other cases resulting in lower distillate production and hence efficiency is lower.

5. Conclusions

The thermal modeling consisting of equating input energy to output energy for different components of the proposed *N* alike fully covered PVT-CPCs integrated active distillation system (double slope) has been performed. The various equations obtained from thermal modeling of the proposed system have been solved for getting analytical characteristic equation for the proposed system. The developed analytical equation for *N* identical fully covered series-connected PVT-CPCs integrated active distiller system (double slope) is also applicable to same number of fully covered PVT-FPCs connected with distiller system (double slope), conventional type *N* identical FPCs connected with solar still (double slope), and passive solar still (double slope). The characteristic curves for various systems namely (case (iv)) passive solar still of double slope type, (case (iii)) conventional FPCs integrated with solar still (double slope), (case (ii) fully covered PVT-FPCs connected with distiller system (double slope), and (case i) PVT-CPCs integrated with solar still (double slope) have been plotted using a computational program written in MATLAB. Comparison for different cases has been done. Based on the comparison, it has been concluded that instantaneous efficiency for the proposed system in case (i) is less than case (iii) whereas more than case (ii) and case (iv).

Acknowledgment

Authors are thankful to Dr. A.P.J. Abdul Kalam Technical University, Lucknow - 226021, UP, India (No. AKTU/Dean-PGSr/2019/CRIP/40) for providing financial support in the accomplishment of the current research work.

Nomenclature

A_{rm} — Area of receiver covered by PV module, m²
A_{am} — Area of aperture covered by PV module, m²
A_g — Area of glass cover, m²
A_b — Area of basin, m²
A_{gE} — Area of east class cover
A_{gW} — Area of west class cover
b — Breath of receiver, m
b_0 — Breath of aperture, m
C_f/C_w — Specific heat of water, J/kg-K
F' — Collector efficiency factor
h_i' — Heat transfer coefficient from bottom of PVT to ambient, W/m²-K
h_0 — Heat transfer coefficient from top of PVT to ambient, W/m²-K
h_{pf} — Heat transfer coefficient from blackened plate to fluid, W/m²-K
h_{rwE} — Radiative heat transfer coefficient from water to inner surface of east glass cover, W/m²-K
h_{rwW} — Radiative heat transfer coefficient from water to inner surface of west glass cover, W/m²-K
h_{cwE} — Convective heat transfer coefficient from water to inner surface of east glass cover, W/m²-K
h_{cwW} — Convective heat transfer coefficient from water to inner surface of west glass cover, W/m²-K
h_{ewE} — Evaporative heat transfer coefficient from water to inner surface of east glass cover, W/m²-K
h_{ewW} — Evaporative heat transfer coefficient from water to inner surface of west glass cover, W/m²-K
$I_b(t)$ — Beam radiation, W/m²
$I(t)$ — Total radiation
$I_{SE}(t)$ — Solar radiation impinging on glass cover facing east
$I_{SW}(t)$ — Solar radiation impinging on glass cover facing west
K_i — Thermal conductivity of insulation, W/m-K
K_g — Thermal conductivity of glass cover, W/m-K
K_p — Thermal conductivity of absorption plate, W/m-K
L — Latent heat, J/kg
L_i — Thickness of insulation, m
L_g — Thickness of glass cover, m
L_r — Total length of receiver area, m
L_a — Total length of aperture area, m
L_{rm} — Length of receiver covered by PV module
L_{am} — Length of aperture covered by PV module
L_p — Thickness of absorption plate, m
$\dot{m}_f$ — Mass flow rate of water, kg/s
PF_2 — Penalty factor due to plate below the module
LHS — Left-hand side
RHS — Right-hand side
T_{fi} — Fluid temperature at collector inlet, °C
T_f — Temperature of fluid in collector, °C
T_a — Ambient temperature, °C
T_{foN} — Outlet water temperature at the end of *N*th PVT–CPC water collector, °C
T_{giE} — Glass temperature at inner surface of east glass cover, °C
T_{giW} — Glass temperature at inner surface of west glass cover, °C
T_{goE} — Glass temperature at outer surface of east glass cover, °C
T_{goW} — Glass temperature at outer surface of west glass cover, °C
$\dot{Q}_{uN}$ — Rate of useful thermal output from *N* identical fully covered PVT-CPC water collectors connected in series, kWh
T — Time, h
T_w — Temperature of water in basin at time *t*, °C
T_a — Ambient temperature, °C
T_{wo} — Water temperature at $t = 0$, °C
$\bar{T}_{cN}$ — Average solar cell temperature
U_{Lm} — Overall heat transfer coefficient from module to ambient, W/m²-K
U_{ta} — Overall heat transfer coefficient from cell to ambient, W/m²-K

U_{tcp} — Overall heat transfer coefficient from solar cell to absorber plate
U_{tca} — Overall heat transfer coefficient from solar cell to ambient
U_{tpa} — Overall heat transfer coefficient from absorber plate to ambient
N — Number of PVT-CPC water collector

Greek Letters

α_c — Absorptivity of the solar cell
ρ — Reflectivity
τ_g — Transmissivity of the glass (fraction)
β_0 — Temperature coefficient of efficiency (K^{-1})
η_c — Solar cell efficiency
η_m — PV module efficiency
$(\alpha\tau)_{eff}$ — Product of effective absorptivity and transmittivity
β — Packing factor of the module
η_0 — Efficiency at standard test condition
ϵ — Emissivity
α' — Absorptivity

Subscripts

g — Glass
w — Water
in — Incoming
out — Outgoing
eff — Effective

References

[1] G.M. Zaki, T. El. Dali, H. El. Shafie, Improved Performance of Solar Still, Proc. First Arab Int. Solar Energy Conference, Kuwait, 1983, pp. 331–335.
[2] S.N. Rai, G.N. Tiwari, Single basin solar still coupled with flat plate collector, Energy Convers. Manage., 23 (1983) 145–149.
[3] Z.S. Abdel-Rehim, A. Lasheen, Experimental and theoretical study of a solar desalination system located in Cairo, Egypt, Desalination, 217 (2007) 52–64.
[4] O.A. Hamadou, K. Abdellatif, Modeling an active solar still for sea water desalination process optimization, Desalination, 354 (2014) 1–8.
[5] A.A. Badran, A.A. Al-Hallaq, I.A. Eyal Salman, M.Z. Odat, A solar still augmented with a flat-plate collector, Desalination, 172 (2005) 227–234.
[6] H. Taghvaei, H. Taghvaei, K. Jafarpur, M.R. Karimi Estahbanati, M. Mansoor Feilizadeh, A. Seddigh Ardekani, A thorough investigation of the effects of water depth on the performance of active solar stills, Desalination, 347 (2014) 77–85.
[7] F. Calise, M.D. d'Accadia, A. Piacentino, A novel solar trigeneration system integrating PVT (photovoltaic/thermal collectors) and SW (seawater) desalination: dynamic simulation and economic assessment, Energy, 67 (2014) 129–148.
[8] A.G.M. Ibrahim, E.E. Allam, S.E. Elshamarka, A modified basin type solar still: experimental performance and economic study, Energy, 93 (2015) 335–342.
[9] S.D. Hendrie, Evaluation of Combined Photovoltaic/Thermal Collectors, Vol. 3, Proceedings of International Conference ISES, Atlanta, GA, USA, 1979, pp. 1865–1869.
[10] E.C. Kern, M.C. Russell, Combined photovoltaic and thermal hybrid collector systems, Proceedings of the 13th IEEE Photovoltaic Specialists, Washington, DC, USA, 1978, pp. 1153–1157.
[11] I. Guarracino, J. Freeman, A. Ramos, S.A. Kalogirou, N.J. Ekins-Daukes, C.N. Markides, Systematic testing of hybrid PV-thermal (PVT) solar collectors in steady state and dynamic outdoor conditions, Appl. Energy, 240 (2019) 1014–1030.
[12] A. Mellor, D.A. Alvarez, I. Guarracino, A. Ramos, A.R. Lacasta, L.F. Llind, A.J. Murrelle, D.J. Pauld, D. Chemisana, C.N. Markides, N.J. Ekins-Daukes, Roadmap for the next-generation of hybrid photovoltaic-thermal solar energy collectors, Sol. Energy, 174 (2018) 386–398.
[13] R. Liang, J. Zhang, L. Ma, Y. Li, Performance evaluation of new type hybrid photovoltaic/thermal solar collector by experimental study, Appl. Therm. Eng., (2014) 487–492, doi: 10.1016/j.applthermaleng.2014.09.075.
[14] W. He, Y. Zhang, J. Ji, Comparative experiment study on photovoltaic and thermal solar system under natural circulation of water, Appl. Therm. Eng., 31 (2011) 3369–3376.
[15] S. Kumar, A. Tiwari, An experimental study of hybrid photovoltaic thermal (PV/T) active solar still, Int. J. Energy Res., 32 (2008) 847–858.
[16] S. Kumar, G.N. Tiwari, Estimation of internal heat transfer coefficients of a hybrid (PV/T) active solar still, Sol. Energy, 83 (2009) 1656–1667.
[17] S. Kumar, G.N. Tiwari, Life cycle cost analysis of single slope hybrid (PV/T) active solar still, Appl. Energy, 86 (2009a) 1995–2004.
[18] S. Kumar, A. Tiwari, Design, fabrication and performance of a hybrid photovoltaic/thermal (PVT) active solar still, Energy Convers. Manage., 51 (2010) 1219–1229.
[19] G. Singh, S. Kumar, G.N. Tiwari, Design, fabrication and performance of a hybrid photovoltaic/thermal (PVT) double slope active solar still, Desalination, 277 (2011) 399–406.
[20] F. Saeedi, F. Sarhaddi, A. Behzadmehr, Optimization of a PV/T (photovoltaic/thermal) active solar still, Energy, 87 (2015) 142–152.
[21] D.B. Singh, G.N. Tiwari, Effect of energy matrices on life cycle cost analysis of partially covered photovoltaic compound parabolic concentrator collector active solar distillation system, Desalination, 397 (2016) 75–91.
[22] D.B. Singh, G.N. Tiwari, Enhancement in energy metrics of double slope solar still by incorporating N identical PVT collectors, Sol. Energy, 143 (2017) 142–161.
[23] D.B. Singh, G.N. Tiwari, Performance analysis of basin type solar stills integrated with N identical photovoltaic thermal (PVT) compound parabolic concentrator (CPC) collectors: a comparative study, Sol. Energy, 142 (2017a) 144–158.
[24] D.B. Singh, G.N. Tiwari, Exergoeconomic, enviroeconomic and productivity analyses of basin type solar stills by incorporating N identical PVT compound parabolic concentrator collectors: a comparative study, Energy Convers. Manage., 135 (2017) 129–147.
[25] H. Prasad, P. Kumar, R.K. Yadav, A. Mallick, N. Kumar, D.B. Singh, Sensitivity analysis of N identical partially covered (50%) PVT compound parabolic concentrator collectors integrated double slope solar distiller unit, Desal. Water Treat., 153 (2019) 54–64.
[26] D.B. Singh, V.K. Dwivedi, G.N. Tiwari, N. Kumar, Analytical characteristic equation of N identical evacuated tubular collectors integrated single slope solar still, Desal. Water Treat., 88 (2017) 41–51.
[27] D.B. Singh, N. Kumar, Harender, S. Kumar, S.K. Sharma, A. Mallick, Effect of depth of water on various efficiencies and productivity of N identical partially covered PVT collectors incorporated single slope solar distiller unit, Desal. Water Treat., 138 (2019) 99–112.
[28] D.B. Singh, G.N. Tiwari, Analytical characteristic equation of N identical evacuated tubular collectors integrated double slope solar still, J. Sol. Energy Eng., 139 (2017) 051003 (11 pages).
[29] M.K. Gaur, G.N. Tiwari, Optimization of number of collectors for integrated PV/T hybrid active solar still, Appl. Energy, 87 (2010) 1763–1772.
[30] M.A. Eltawil, Z.M. Omara, Enhancing the solar still performance using solar photovoltaic, flat plate collector and hot air, Desalination, 349 (2014) 1–9.
[31] K. Rabhi, R. Nciria, F. Nasria, C. Alia, H.B. Bachae, Experimental performance analysis of a modified single-basin single-slope

solar still with pin fins absorber and condenser, Desalination, 416 (2017) 86–93.
[32] S.W. Sharshir, G. Peng, N. Yang, M.A. Eltawil, M.K.A. Ali, A.E. Kabeel, A hybrid desalination system using humidification-dehumidification and solar stills integrated with evacuated solar water heater, Energy Convers. Manage., 124 (2016) 287–296.
[33] J.A.A. Navarro, M.C. Téllez, M.A.R. Martínez, G.P. Silvar, F.C.M. Tejeda, Computational thermal analysis of a double slope solar still using Energy2D, Desal. Water Treat., 151 (2019) 26–33.
[34] S.K. Sharma, A. Mallick, S.K. Gupta, D.B. Singh, N. Kumar, G.N. Tiwari, Characteristic equation development for double slope solar distiller unit augmented with N identical parabolic concentrator integrated evacuated tubular collectors, Desal. Water Treat., (2020), doi: 10.5004/dwt.2020.25394.
[35] C. Haiping, G. Xinxin, Z. Heng, L. Yang, L. Haowen, B. Yuegang, Experimental study on a flash tank integrated with low concentrating PV/T (FT-LCPVT) hybrid system for desalination, Appl. Therm. Eng., 159 (2019) 113874
[36] J.A. Duffie, W.A. Beckman, Solar Engineering of Thermal Processes, John Wiley and Sons, New York, 1991.
[37] G.N. Tiwari, Solar Energy: Fundamentals, Design, Modeling and Applications, Narosa Publishing House, New Delhi, 2004.
[38] D.L. Evans, Simplified method for predicting PV array output, Sol. Energy, 27 (1981) 555–560.
[39] T. Schott, Operational Temperatures of PV Modules, Proceedings of 6th PV Solar Energy Conference, 1985, 392–396.
[40] R. Tripathi, G.N. Tiwari, Annual performance evaluation (energy and exergy) of fully covered concentrated photovoltaic thermal (PVT) water collector: an experimental validation, Sol. Energy, 146 (2017) 180–190.
[41] V.K. Dwivedi, G.N. Tiwari, Comparison of internal heat transfer coefficients in passive solar stills by different thermal models: an experimental validation, Desalination, 246 (2009) 304–318.
[42] S. Kumar, G.N. Tiwari, Estimation of convective mass transfers in solar distillation system, Sol. Energy, 57 (1996) 459–464.
[43] R.V. Dunkle, Solar Water Distillation, the Roof Type Solar Still and a Multi Effect Diffusion Still, International Developments in Heat Transfer, ASME, Proc. Int. Heat Transfer, Part V, University of Colorado, 1961, 895 pp.
[44] Z. Chen, X. Ge, X. Sun, L. Bar, Y.X. Miao, Natural Convection Heat Transfer Across Air Layers at Various Angles of Inclination, Engineering Thermophysics, 1984, pp. 211–220.
[45] R.S. Adhikari, A. Kumar, A. Kumar, Estimation of mass transfer rates in solar stills, Int. J. Energy Res., 14 (1990) 737–744.
[46] H. Zheng, X. Zhang, J. Zhang, Y. Wu, A group of improved heat and mass transfer correlations in solar stills, Energy Convers. Manage., 43 (2001) 2469–2478.
[47] J.A. Clark, The steady state performance of a solar still, Sol. Energy, 44 (1990) 43–49.

Appendix-A

$$U_{\text{tca}}=\left[\frac{1}{h_0}+\frac{L_g}{K_g}\right]^{-1};\quad U_{\text{tcp}}=\left[\frac{1}{h_i}+\frac{L_g}{K_g}\right]^{-1};\quad h_0=5.7+3.8V,\quad \text{Wm}^{-2}\text{K}^{-1}; \tag{A1}$$

$$h_i=5.7,\text{Wm}^{-2}\text{K}^{-1};\quad U_{\text{tpa}}=\left[\frac{1}{U_{\text{tca}}}+\frac{1}{U_{\text{tcp}}}\right]^{-1}+\left[\frac{1}{h_i'}+\frac{1}{h_{\text{pf}}}+\frac{L_i}{K_i}\right]^{-1}; \tag{A2}$$

$$h_i'=2.8+3V',\text{Wm}^{-2}\text{K}^{-1};\quad U_{L1}=\frac{U_{\text{tcp}}U_{\text{tca}}}{U_{\text{tcp}}+U_{\text{tca}}};\quad U_{L2}=U_{L1}+U_{\text{tpa}}; \tag{A3}$$

$$U_{\text{Lm}}=\frac{h_{\text{pf}}U_{L2}}{F'h_{\text{pf}}+U_{L2}};\quad \text{PF}_1=\frac{U_{\text{tcp}}}{U_{\text{tcp}}+U_{\text{tca}}};\quad \text{PF}_2=\frac{h_{\text{pf}}}{F'h_{\text{pf}}+U_{L2}}; \tag{A4}$$

$$\left(\alpha\tau\right)_{\text{1eff}}=\rho\left(\alpha_c-\eta_c\right)\tau_g\beta_c\frac{A_{\text{am}}}{A_{\text{rm}}};\quad \left(\alpha\tau\right)_{\text{2eff}}=\rho\alpha_p\tau_g^2\left(1-\beta\right)\frac{A_{\text{am}}}{A_{\text{rm}}}; \tag{A5}$$

$$\left(\alpha\tau\right)_{\text{meff}}=\left[\left(\alpha\tau\right)_{\text{1eff}}+\text{PF}_1\left(\alpha\tau\right)_{\text{2eff}}\right]; \tag{A6}$$

$$B=\left(h_{\text{1wE}}U_2+h_{\text{1wW}}h_{\text{EW}}A_{\text{gW}}\right)\frac{A_b}{2};\quad U_2=h_{\text{1wW}}\frac{A_b}{2}+h_{\text{EW}}A_{\text{gW}}+U_{\text{cW}}A_{\text{gW}}; \tag{A7}$$

$$H=U_1U_2-h_{\text{EW}}^2A_{\text{gE}}A_{\text{gW}};\quad U_1=h_{\text{1wE}}\frac{A_b}{2}+h_{\text{EW}}A_{\text{gE}}+U_{\text{cE}}A_{\text{gE}}; \tag{A8}$$

$$A=C_1U_2+C_2;\quad C_2=\alpha_gI_{\text{SW}}\left(t\right)h_{\text{EW}}A_{\text{gE}}A_{\text{gW}}+U_{\text{cW}}h_{\text{EW}}A_{\text{gE}}A_{\text{gW}}T_a; \tag{A9}$$

$$C_1 = \alpha'_g I_{SE}(t) A_{gE} + U_{cE} A_{gE} T_a \text{ and } C'_1 = \alpha'_g I_{SW}(t) A_{gW} + U_{cW} A_{gW} T_a \tag{A10}$$

$$B' = \left(h_{1wW} U_1 + h_{1wE} h_{EW} A_{gE}\right) \frac{A_b}{2};\ A' = C'_1 U_1 + C'_2; \tag{A11}$$

$$C'_2 = \alpha'_g I_{SE}(t) h_{EW} A_{gE} A_{gW} + U_{cE} h_{EW} A_{gE} A_{gW} T_a; \tag{A12}$$

$$E_1 = U_{cE}\left[h_{EW} + h_{1wW}\left(\frac{A_b}{2A_{gW}}\right)\right] A_{gE} A_{gW};\ E_2 = U_{cW}\left[h_{EW} + U_{cE}\right] A_{gE} A_{gW}; \tag{A13}$$

$$E'_1 = U_{cW}\left[h_{EW} + h_{1wE}\left(\frac{A_b}{2A_{gE}}\right)\right] A_{gE} A_{gW};\ E'_2 = U_{cE}\left[h_{EW} + U_{cW}\right] A_{gE} A_{gW}; \tag{A14}$$

$$H'_{22} = \left(\frac{2H}{A_b}\right)\left\{U_b A_b + N\left(A_m F_{Rm}\right) U_{Lm}\right\}; \tag{A15}$$

$$H'_{11} = H_1 + H_2 + H_3 + H_4;\ H_1 = \left(U_{cE} A_{gE} + U_{cW} A_{gW}\right) \frac{A_b}{2} h_{1wE} h_{1wW}; \tag{A16}$$

$$H_2 = \left(h_{1wE} U_{cE} + h_{1wW} U_{cW}\right) h_{EW} A_{gE} A_g;\ H_3 = \left(h_{1wE} + h_{1wW}\right) U_{cE} U_{cW} A_{gE} A_g; \tag{A17}$$

$$H_4 = \left(h_{1wE} U_{cE} + h_{1wW} U_{cW}\right) h_{EW} A_{gE} A_g; \tag{A18}$$

$$K_{1E} = \alpha'_g h_{1wE} A_{gE} A_{gW}\left[h_{1wW}\left(\frac{A_b}{2A_{gW}}\right) + h_{EW}\left(1 + \frac{h_{1wW}}{h_{1wE}}\right) + U_{cW}\right]; \tag{A19}$$

$$K_{1W} = \alpha'_g h_{1wW} A_{gE} A_{gW}\left[h_{1wE}\left(\frac{A_b}{2A_{gE}}\right) + h_{EW}\left(1 + \frac{h_{1wE}}{h_{1wW}}\right) + U_{cE}\right];\ \alpha_{wb} = \left(\alpha'_w + 2\alpha'_b h_1\right) H \tag{A20}$$

$$K'_{1E} = \alpha'_g h_{ewE} A_{gE} A_{gW}\left[h_{ewW}\left(\frac{A_b}{2A_{gW}}\right) + h_{EW}\left(1 + \frac{h_{ewW}}{h_{ewE}}\right) + U_{cW}\right]; \tag{A21}$$

$$K'_{1W} = \alpha'_g h_{ewW} A_{gE} A_{gW}\left[h_{ewE}\left(\frac{A_b}{2A_{gE}}\right) + h_{EW}\left(1 + \frac{h_{1wE}}{h_{1wW}}\right) + U_{cE}\right]; \tag{A22}$$

$$h_{ewE} = 16.273 \times 10^{-3} h_{cwE}\left[\frac{P_w - P_{giE}}{T_w - T_{giE}}\right] [40]; \tag{A23}$$

$$h_{ewW} = 16.273 \times 10^{-3} h_{cwW}\left[\frac{P_w - P_{giW}}{T_w - T_{giW}}\right] [40]; \tag{A24}$$

$$h_{cwE} = 0.884\left[\left(T_w - T_{giE}\right) + \frac{\left(P_w - P_{giE}\right)\left(T_w + 273\right)}{268.9 \times 10^3 - P_w}\right]^{\frac{1}{3}} [41] \tag{A25}$$

$$h_{\mathrm{cwW}} = 0.884\left[\left(T_w - T_{\mathrm{giW}}\right) + \frac{\left(P_w - P_{\mathrm{giW}}\right)\left(T_w + 273\right)}{268.9\times10^3 - P_w}\right]^{\frac{1}{3}} \text{ [41]} \tag{A26}$$

$$P_w = \exp\left[25.317 - \frac{5{,}144}{T_w + 273}\right]; \tag{A27}$$

$$P_{\mathrm{giE}} = \exp\left[25.317 - \frac{5{,}144}{T_{\mathrm{giE}} + 273}\right]; \quad P_{\mathrm{giW}} = \exp\left[25.317 - \frac{5{,}144}{T_{\mathrm{giW}} + 273}\right]; \tag{A28}$$

$$h_{\mathrm{rw}} = \left(0.82\times5.67\times10^{-8}\right)\left[(T_w + 273)^2 + (T_{\mathrm{gi}} + 273)^2\right]\left[T_w + T_{\mathrm{gi}} + 546\right]; \tag{A29}$$

$$h_{\mathrm{EW}} = 0.034\times5.67\times10^{-8}\left[\left(T_{\mathrm{giE}} + 273\right)^2 + \left(T_{\mathrm{giW}} + 273\right)^2\right]\left[T_{\mathrm{giE}} + T_{\mathrm{giW}} + 546\right] \tag{A30}$$